AGU PUBLICATIONS

JGR

Journal of Geophysical Research: Atmospheres

RESEARCH ARTICLE
10.1002/2016JD025667

Key Points:
- Microphysical properties of thin liquid water clouds
- Improving statistical retrieval accuracy by combining microwave and infrared regime
- Evaluation of retrieval performance in a radiative closure study with real measurements

Correspondence to:
T. Marke,
tmarke@meteo.uni-koeln.de

Citation:
Marke, T., K. Ebell, U. Löhnert, and D. D. Turner (2016), Statistical retrieval of thin liquid cloud microphysical properties using ground-based infrared and microwave observations, *J. Geophys. Res. Atmos.*, *121*, 14,558–14,573, doi:10.1002/2016JD025667.

Received 18 JUL 2016
Accepted 17 NOV 2016
Accepted article online 23 NOV 2016
Published online 20 DEC 2016

Statistical retrieval of thin liquid cloud microphysical properties using ground-based infrared and microwave observations

Tobias Marke[1], Kerstin Ebell[1], Ulrich Löhnert[1], and David D. Turner[2]

[1]Institute for Geophysics and Meteorology, University of Cologne, Cologne, Germany, [2]National Severe Storms Laboratory, Norman, Oklahoma, USA

Abstract In this article, liquid water cloud microphysical properties are retrieved by a combination of microwave and infrared ground-based observations. Clouds containing liquid water are frequently occurring in most climate regimes and play a significant role in terms of interaction with radiation. Small perturbations in the amount of liquid water contained in the cloud can cause large variations in the radiative fluxes. This effect is enhanced for thin clouds (liquid water path, LWP <100 g/m^2), which makes accurate retrieval information of the cloud properties crucial. Due to large relative errors in retrieving low LWP values from observations in the microwave domain and a high sensitivity for infrared methods when the LWP is low, a synergistic retrieval based on a neural network approach is built to estimate both LWP and cloud effective radius (r_{eff}). These statistical retrievals can be applied without high computational demand but imply constraints like prior information on cloud phase and cloud layering. The neural network retrievals are able to retrieve LWP and r_{eff} for thin clouds with a mean relative error of 9% and 17%, respectively. This is demonstrated using synthetic observations of a microwave radiometer (MWR) and a spectrally highly resolved infrared interferometer. The accuracy and robustness of the synergistic retrievals is confirmed by a low bias in a radiative closure study for the downwelling shortwave flux, even for marginally invalid scenes. Also, broadband infrared radiance observations, in combination with the MWR, have the potential to retrieve LWP with a higher accuracy than a MWR-only retrieval.

1. Introduction

Assessing the impact of clouds on the global circulation represents a major task in improving climate models. Quoting the fifth assessment report (AR5), the Intergovernmental Panel on Climate Change (IPCC) states that clouds and their associated macrophysical and microphysical processes are still responsible for large uncertainties in the estimation and interpretation of the Earth's energy budget [*Intergovernmental Panel on Climate Change*, 2013]. Clouds drive the atmospheric circulation through complex interactions with solar and thermal fluxes from the surface and the atmosphere [*Stephens*, 2005]. In situations with a low liquid water path (LWP), the radiative fluxes are especially sensitive to liquid water variations [*Turner et al.*, 2007b; *Sengupta et al.*, 2003]. Thus, special emphasis needs to be put on thin liquid water clouds, which are here defined as clouds containing low amounts of liquid water (LWP below 100g/m^2). Furthermore, *Turner et al.* [2007a] revealed that a high frequency of occurrence (between 43% and 67%) of thin liquid water clouds can be observed in most climate regimes, including the Arctic (Barrow, Alaska), a continental midlatitude site (Lamont, Oklahoma), and the tropical Western Pacific (Darwin, Australia). Thus, in order to better represent thin liquid water clouds and their impact on radiative fluxes and heating rates in climate models, it is extremely important to develop instruments and retrieval algorithms that can be used to accurately derive properties of these clouds like LWP and cloud droplet effective radius (r_{eff}) [*Löhnert and Crewell*, 2003].

Microphysical and optical cloud properties, such as LWP and r_{eff}, can be used to describe the interactions of clouds with radiation [*Hu and Stamnes*, 1993; *Stephens*, 1978]. Most notably, the impact of clouds on the radiative flux is mainly dependent on the total amount of condensed water contained in the cloud [*Turner et al.*, 2007a]. The effective radius is also valuable for understanding the mechanisms of cloud formation, dissipation, and interactions with aerosol and drizzle [*Kubar et al.*, 2009].

Ground-based remote sensing instruments, like active cloud radars or passive instruments, are commonly used for observing liquid water clouds [*Turner et al.*, 2007b]. Typically, automated observation methods are

able to obtain long-term records of cloud properties with a high temporal resolution from the radiative energy that is emitted, transmitted, or reflected by the cloud. Passive remote sensing instruments are preferable because they are typically more affordable than active remote sensors [*Crewell et al.*, 2009] but do not provide vertical cloud information.

Comparisons of state-of-the-art retrieval methods show large discrepancies in retrieving LWP and r_{eff} for liquid water clouds. *Turner et al.* [2007b] evaluated different MWR-based LWP algorithms for a cloudy case with a LWP less than 100g/m^2 and found a spread of 40g/m^2 between the LWP algorithms, which was primarily due to the retrieval technique and the assumptions used in the methods. This result agrees with the conclusions of *Marchand et al.* [2003] and *Sengupta et al.* [2003], both of which included random uncertainties in the microwave brightness temperatures in the retrieval. This emphasizes the demand for improving the accuracy of retrieval algorithms for thin clouds.

The microwave radiometer (MWR) is the most common single-instrument approach to retrieve LWP [*Löhnert and Crewell*, 2003; *Liljegren et al.*, 2001] and has been used for decades [e.g., *Westwater*, 1978]. Observations in the microwave region can be used to retrieve LWP, because of the semitransparency of clouds [*Löhnert et al.*, 2004] and the increase of the liquid water contribution in the emitted signal with higher frequency [*Crewell et al.*, 2009]. The MWR is able to retrieve wide ranges of LWP without saturation but with a LWP retrieval error of around 20–30g/m^2 [*Marchand et al.*, 2003; *Löhnert and Crewell*, 2003]. This results in high relative uncertainties for clouds with low LWP values.

Similar to the passive MWR, also, techniques in the infrared domain make use of the energy emitted by the atmosphere to gain information on cloud properties. If the cloud is single layered and contains low amounts of liquid water, the infrared methods are able to obtain simultaneous estimates of LWP and r_{eff} [*Turner et al.*, 2007b]. The infrared domain offers a significantly higher sensitivity to changes in LWP for low amounts of cloud liquid water than the MWR [*Turner*, 2007]. Note that the infrared observations are also sensitive toward ice clouds. Thus, prior information on the cloud phase must be available, because an incorrect phase determination can lead to errors in the estimates of the single-scattering properties [*Turner et al.*, 2003]. The distinction between liquid water and ice can be achieved by taking advantage of differences in the refraction index of ice and water in the highly resolved infrared spectrum between 11 and 19μm for a low amount of precipitable water vapor (PWV<1 cm, according to *Turner et al.* [2003]). This prevents Atmospheric Emitted Radiance Interferometer (AERI) observations from being used in most midlatitude and all tropical locations. Thus, using active remote sensors and an algorithm like the cloud classification scheme Cloudnet [*Illingworth et al.*, 2007], as done in the present study, provides a much more robust and consistent cloud phase identification over the entire PWV range.

Since the interaction of atmospheric constituents with radiation changes with wavelength, spectrally diverse measurements contain different information about the atmospheric composition. Therefore, the optimal instrument and frequency combination needs to be determined [*Löhnert et al.*, 2004]. Ground-based instruments in the infrared domain have the advantage of high sensitivities to clouds with small LWP, when on the other side the uncertainty in the MWR retrievals is relatively large. Conversely, the infrared signal saturates at larger amounts of LWP (around 60g/m^2 [*Turner*, 2007]), leading to large uncertainties in the infrared retrievals. Hence, we focus on LWP and r_{eff} retrievals using a combination of ground-based microwave and infrared observations. These synergistic LWP retrievals show a high sensitivity for low-LWP situations and are still able to retrieve LWP over the entire dynamic range.

A combined LWP retrieval using the microwave and infrared spectral region has been developed by *Turner* [2007] and showed improved skills in retrieving LWP relative to a MWR-only retrieval approach. That retrieval algorithm was developed for mixed-phase clouds and used the optimal estimation approach [e.g., *Rodgers*, 2000]. Such physical algorithms are rather complex and computationally expensive, requiring vertical profiles of temperature and humidity as input (e.g., from radiosonde data). This study focuses on statistical retrievals for LWP and r_{eff} , i.e., a neural network approach, where vertical profiles are not required and therefore the derivation of the retrievals is independent of the times of radiosonde ascents. Moreover, the statistical retrievals are easy to handle: applying the retrievals only requires a matrix multiplication of the measured quantity together with the one-time-derived retrieval coefficients. However, it is not readily evident that a statistical retrieval can be derived with a similar accuracy than the physical retrieval, due to the nonlinear response of the downwelling radiation to increasing LWP in the infrared domain [*Turner*, 2007]. Hereby a neural network approach is chosen to accomplish this goal, and the scientific objectives of this study are

Table 1. Wavenumber Ranges for AERI Microwindows

#	Wavenumber (cm^{-1})	#	Wavenumber (cm^{-1})
1	770.9–774.8	8	872.2–877.5
2	785.9–790.7	9	891.9–895.8
3	809.0–812.9	10	898.2–905.4
4	815.3–824.4	11	929.6–939.7
5	828.3–834.6	12	959.9–964.3
6	842.8–848.1	13	985.0–998.0
7	860.1–864.0		

as follows: performance evaluation for single-instrument and synergy retrievals in the microwave and infrared domains using synthetic data, comparison of the retrievals using spectrally highly resolved or broadband infrared observations, and retrieval validation in a radiative closure study using real measurements.

In the next section, the instruments that are deployed in this study and their specifications are described. In section 3, the methodology is presented including the retrieval development and the compilation of synthetic data for retrieval training and testing. In section 4, the retrievals are tested with the synthetic data, while section 5 deals with the application of the retrievals to real measurements in a radiative closure study.

2. Instruments

This study includes three types of state-of-the-art passive ground-based remote sensing instruments: a microwave Humidity And Temperature PROfiler (HATPRO-MWR), two broadband infrared radiometers (IRRs), and the infrared Atmospheric Emitted Radiance Interferometer (AERI). In the following, the basic principles and characteristics of each instrument are briefly specified. The measurements are taken from the Jülich Observatory for Cloud Evolution (JOYCE) [*Löhnert et al.*, 2015]. JOYCE is operated jointly by the University of Cologne, the Research Centre Jülich, and the Transregional Collaborative Research Centre "Patterns in Soil-Vegetation-Atmosphere Systems: Monitoring, Modelling and Data Assimilation." The scientific goal of JOYCE is to observe the spatial and temporal variability of atmospheric water cycle variables.

2.1. Infrared Interferometer AERI

The Atmospheric Emitted Radiance Interferometer (AERI) is an operational ground-based spectrometer. The AERI measures the downwelling infrared radiance every 16–17 s at approximately $1cm^{-1}$ resolution from 520 to $3000cm^{-1}$ (corresponding to 3.3–19.2μm), with a narrow zenith field of view. Since there is no significant infrared emission from space in the downwelling radiance, the entire signal is provided by emission from the atmosphere. Two detectors are used in a "sandwich" configuration, to provide the needed sensitivity across the entire spectral range [*Knuteson et al.*, 2004a]. Approximately 2500 spectral channels for each of its two detectors are provided. This is accomplished by measuring the interference pattern created by the interferometer. The two well-characterized blackbodies (one at ambient air temperature and the other fixed at 60°C) and the application of a nonlinearity correction for the detectors result in the radiometric accuracy of the radiance measurements being better than 1% of the ambient radiance [*Knuteson et al.*, 2004b].

Turner [2005] has shown that the AERI high spectral resolution observations can be used to retrieve microphysical cloud properties, utilizing "microwindows" between gaseous absorption lines and thereby minimizing the effects of atmospheric gases. In this study, 13 microwindows are used (Table 1), which are described in *Turner* [2005]. They are located between $770.9cm^{-1}$ (13.0μm) and $998cm^{-1}$ (10.0μm), which is a spectral region with a high sensitivity to liquid water. The uncertainty in the AERI observations is less than $1mW/(m^2\ srcm^{-1})$. The study of *Turner* [2007] shows that the AERI possesses a high sensitivity to changes in LWP until the LWP increases above 60 g/m^2. At LWP values below $60g/m^2$, the sensitivity of the downwelling radiance to changes in LWP is higher than the AERI uncertainty. For optically thicker clouds, a further rise in the LWP produces only a slightly increase in the infrared radiance, which can no longer be distinguished from the measurement noise.

2.2. Microwave and Infrared Radiometers

The Humidity And Temperature PROfiler (HATPRO) at JOYCE consists of a passive microwave radiometer utilizing direct detection receivers. Usually, a two-channel statistical or physical retrieval is applied to derive LWP using observations of the downwelling microwave radiance at 23.8 and 31.4 GHz [e.g., *Liljegren et al.*, 2001].

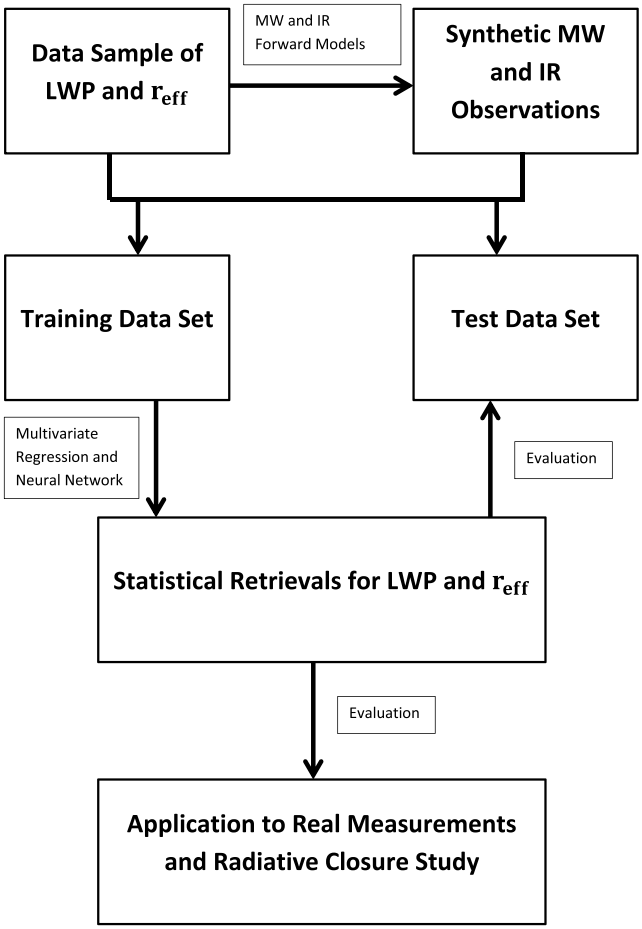

Figure 1. Flow chart of the study setup.

The former frequency is on the wing of the 22.2 GHz water vapor absorption line, and the latter frequency is located in an atmospheric window, where the signal is dominated by liquid water emission when clouds are in the instrument's field of view. The estimated error in the two-channel MWR retrieved LWP is usually considered to be at least 20–30g/m^2 because of uncertainties in the microwave absorption model, the applied retrieval method, and the measurement accuracy [*Turner et al.*, 2007b]. Considering the low LWP values of thin clouds (below 100g/m^2), this uncertainty converts into relative errors being 20% or more.

The MWR measures the brightness temperatures (TB) at seven channels in the K band from 22 GHz to 32 GHz and at seven channels also in the V band from 52 GHz to 58 GHz. The instrument was designed to observe liquid water path with a high temporal resolution up to 1 s [*Rose et al.*, 2005]. In this study, only zenith observations of the seven K-band channels with a 1 s temporal resolution are taken into account. The zenith measurements alternate with full hemispheric scans for temperature profiling. In contrast to the infrared domain, the absorption has no dependence on the droplet size distribution (DSD) and thus r_{eff}, since the cloud droplets are significantly smaller than the wavelength and are therefore located in the Rayleigh scattering regime [*Crewell et al.*, 2009].

In addition, the microwave radiometer is equipped with two broadband infrared radiometers (IRRs). The first IRR has a maximum sensitivity at around 11.1μm (bandpass 10.2–11.9μm), and the second one provides a maximum sensitivity at around 12μm (bandpass 11.1–12.8μm), which correspond to wavelength ranges of 840.3–980.4cm^{-1} and 781.3–900.9cm^{-1}, respectively. The accuracy is denoted to be about 1 K. The IRR wavelength bands are located in an atmospheric window where the measured longwave radiation is dominated by clouds and saturation is expected to be around 40g/m^2. The adjustment of the elevation angle of the IRRs is linked to the MWR. The IRRs in this study are used to examine the potential of broadband infrared measurements to retrieve cloud properties, in comparison to spectrally highly resolved observations of the AERI, which are of much higher cost and have a higher calibration demand.

2.3. Shortwave Broadband Measurements

For the radiative closure study in the last part of this study, the Kipp & Zonen CMP 21 pyranometer is used to measure the downwelling broadband hemispheric irradiance in the solar spectrum (285 to 2800 nm) with a 5 s temporal resolution. The instrument is bias corrected for a nighttime offset and the cosine effect. The error estimation also includes the sensitivity of the data logger and its temperature dependence.

3. Methodology

The methodology of this study is summarized in Figure 1. First, a data sample of single-layer liquid water cloud properties is generated. Using this data sample, MWR and IRR brightness temperatures, as well as

AERI radiances, are simulated. The combined cloud property and measurement data set is separated into a training and test data set. Statistical retrievals are developed based on the training data set, which are in turn evaluated with the test data set. Finally, the retrievals are applied to real measurements. Each step will be explained in detail in the following.

3.1. Data Sample of Single-Layer Liquid Water Cloud Properties

For the derivation of the statistical retrievals, a training and test data sample containing only cases of single-layer liquid water clouds is prepared. These samples include the LWP and the cloud layer mean r_{eff}. In addition to LWP and r_{eff}, a thermodynamic profile of temperature, pressure, and humidity are needed to simulate MWR, AERI, and IRR observations, which are then used for retrieval development. This compiled data set is assumed to represent the characteristics of single-layer water clouds at JOYCE. In order to create the data set of LWP and r_{eff}, cloud radar and MWR measurements are used in combination with simple radar-MWR retrievals for retrieving a r_{eff} training data set. In order to ensure that the training data set contains only the desired single-layer liquid water clouds and the measured signal is not influenced by any other clouds, information on cloud phase and cloud layers is required. Both cloud phase and number of cloud layers can be determined by using the Cloudnet classification product. If the Cloudnet product is not available, a different cloud classification, involving radar and lidar measurements, needs to be applied to allow for a physical interpretation of the retrieval results.

In order to create this data set of LWP and r_{eff}, JOYCE measurements in combination with cloud radar reflectivity/MWR methods are used. First, single-layer liquid clouds are detected using the Cloudnet classification product. The core instruments for Cloudnet are a Doppler cloud radar, a lidar ceilometer, a multiwavelength microwave radiometer, and a rain gauge. The classification product provides vertically resolved information on the cloud phase averaged for 30 s. In addition, profiles of temperature, pressure, and humidity are included, which are from either the European Centre for Medium-Range Weather Forecasting (ECMWF) model or the numerical weather prediction model COSMO-DE [*Baldauf and other*, 2011]. Further details of the Cloudnet product can be found in *Illingworth et al.* [2007].

The backscatter targets in each radar/lidar pixel are categorized into a number of different classes, including precipitation. If drizzle or rain is present, the cloud radar reflectivity is dominated by large drops and simple cloud radar reflectivity/MWR methods are not applicable. Thus, in this study, only nonprecipitating clouds are included and determined by using the Cloudnet approach. The identification of clouds containing drizzle can also be achieved by using thresholds in the radar reflectivity only [*Krasnov and Russchenberg*, 2002] or as a ratio to ceilometer extinction [*Frisch et al.*, 1995] to discriminate drizzle-free clouds. Furthermore, clouds must be present for at least 2min in order to avoid spurious cloud detection and to ensure full cloud cover in the instrument's field of view.

With the previous described Cloudnet classification, 5780 cases (30 s averages) of single-layer liquid water clouds without precipitation are identified for the JOYCE site in the period of 13 March to 31 December 2012. For the liquid water path, the Cloudnet-derived LWP is used, which is based on a statistical retrieval using microwave observations. Such retrievals may provide physically unrealistic negative values, which have been excluded in this data sample. The LWP distribution shows the expected high occurrence of low LWP values for the liquid water clouds with a median of 28.6g/m^2 (not shown). Clouds with a LWP below 100g/m^2, which represent the cloud type of main interest in this study, account for 87.9% of all observed single-layer liquid cloud profiles in this period. Note that the statistical retrieval can only be as good as the training data set, which is assumed to encompass the full range of atmospheric conditions. This results in site and cloud type-specific training data set, which could be extended to more cloud types in future studies (mixed-phase clouds). If other sites exhibit similar atmospheric conditions, it is sensible to apply the developed retrievals at these sites. Otherwise, new retrieval coefficients based on a more appropriate training data set have to be found.

In order to have an estimate of mean layer r_{eff} and vertical information on these cloud properties needed for the forward simulations, a cloud radar/microwave radiometer method is deployed. A homogeneous mixing model, described in *Knist* [2014], is used to derive profiles of LWC and r_{eff} from the cloud layer mean r_{eff}. Homogeneous mixing is described by a faster mixing process than the effects of evaporation. In this case, evaporation reduces uniformly the DSD and the number concentration and the DSD shape parameter does not change. If this process occurs, the microphysical cloud properties consequently change according to *Boers et al.* [2006] and the impact of mixing accounts for the vertical variation in the radar reflectivity [*Knist*, 2014].

Table 2. Main Cloud Properties of the Data Sample

Property	Mean ± SD	Median	Minimum	Maximum
Base height	1769.6 ± 889.9 m	1985.9 m	143.9 m	4000.5 m
Thickness	337.9 ± 185.6 m	287.8 m	86.3 m	1870.8 m
LWP	51.2 ± 71.1 g/m^2	28.6g/m^2	0.02g/m^2	1032.2g/m^2
LWC	0.2 ± 0.2 g/m^3	0.2g/m^3	$1.6 \cdot 10^{-4}$ g/m^3	1.4g/m^3
r_{eff}	6.3 ± 2.2 µm	4.0µm	1.0µm	32.4µm

For the homogeneous mixing model a gamma DSD is applied, which is frequently used in liquid cloud studies [*Miles et al.*, 2000] and results in the following equations for the LWC and r_{eff} as used in *Knist* [2014]:

$$\mathrm{LWC(h)} = \mathrm{LWP}\frac{Z^{1/2}(h)}{\sum_{i=0}^{n} Z^{1/2}(h_i)\Delta h}, \tag{1}$$

where h is the height above cloud base and Δh is the radar range gate. The radar reflectivity Z is summed up from the base to the top of the cloud. The LWP is taken from the Cloudnet output and is also used to derive the r_{eff} in this approach:

$$r_{\mathrm{eff}}(h) = k_{R_\nu}\left(\frac{\pi\rho_w \sum_{i=0}^{n} Z^{1/2}(h_i)}{48\,\mathrm{LWP}}\right)^{1/3} Z^{1/6}(h), \tag{2}$$

$$k_{R_\nu} = \left(\frac{(\nu+2)^3}{((\nu+3)(\nu+4)(\nu+5))}\right)^{1/3}, \quad \nu = 8.7\,. \tag{3}$$

The r_{eff} derivation depends on the DSD shape parameter ν through the coefficient k_{R_ν}. In this study, continental single-layer liquid water clouds are examined, which are expected to have larger droplet concentrations and smaller particle sizes. Referring to several experimental data of such cloud types, the reported mean value of $\nu = 8.7$ for the gamma DSD shape parameter is used according to *Miles et al.* [2000].

In this study, mean values of the derived data sample are 4.2µm for r_{eff} and 0.2g/m^3 for LWC. In *Chiu et al.* [2012], who also used the radar reflectivity for deriving r_{eff}, the distribution of the effective radius peaks at 6–8µm for single-layer liquid water clouds. The reason for the smaller derived values in this study is most likely the uncertainty in LWP. Since negative values from the MWR-derived LWP are not considered for the radiative transfer calculations, the mean value of the data set is higher than the "true" mean value. This can introduce a negative bias in retrieving r_{eff} in a LWP/Z relationship-based method, where r_{eff} is inversely proportional to the LWP. A further source of errors is the assumption on the droplet concentration, which is determined by the constant choice of ν and can cause large uncertainties [*Zhao et al.*, 2012]. In order to increase the possible range of the r_{eff} values, the variability of the data set has been increased by 50%, resulting in an increased mean value of 6.3µm. An overview of the characteristics of the cloud data sample is given in Table 2.

3.2. Simulated Microwave and Infrared Observations

In this section, the infrared and microwave forward models to simulate the MWR, AERI, and IRR observations using the previously described data sample are presented.

3.2.1. Infrared Forward Model

The LBLDIS [*Turner et al.*, 2003] forward model combines a Line-by-Line Radiative Transfer Model (LBLRTM) [*Clough et al.*, 1992], computing infrared atmospheric emission spectra for gases and the Discrete Ordinate Radiate Transfer (DISORT) [*Stamnes et al.*, 1988] model, accounting for the scattering and absorption properties of the cloud. Input variables are, in addition to the cloud microphysical properties of the data sample, thermodynamic profiles of temperature (T), pressure (p), and humidity (q), which are taken from COSMO-DE model output. Figure 2 shows the simulated AERI spectrum for a clear-sky case and the high sensitivity to increasing LWP values. But also, the saturation effect for higher LWP values is visible. For the simulated infrared observations, the corresponding AERI spectral resolution using the previous described microwindows (grey bars, Figure 2) and IRR spectral response functions (dashed blue and red lines in Figure 2) are taken into account.

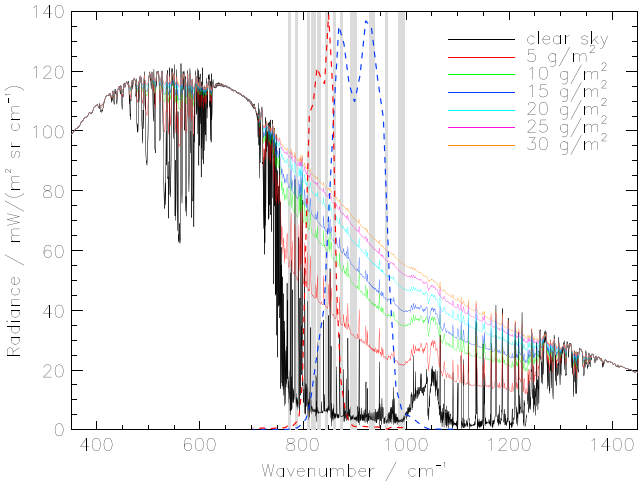

Figure 2. Simulated AERI radiances using LBLDIS for clear sky (solid black line) and different LWP ranging from 5 to 30g/m^2 (solid colored lines) with constant effective radius (r_{eff} = 7 μm). Grey bars denote the 13 microwindows and dashed colored lines the IRR spectral response functions.

3.2.2. Microwave Forward Model

A radiative transfer operator is used to simulate the brightness temperatures for the seven MWR frequencies f_i between 22 and 32 GHz *Löhnert et al.* [2004].

$$TB_i = RTO(\mathbf{T}, \mathbf{p}, \mathbf{q}, \mathbf{LWC}, f_i), \quad (4)$$

with i from 1 to 7, denoting the MWR frequencies, and the COSMO-DE given atmospheric state vectors (**T**, **p**, **q**, and **LWC**).

The forward model performing the radiative transfer calculation (RTO is the radiative transfer operator) is only valid for nonscattering cases. Therefore, the approximation is only applicable for nonprecipitating clouds and for frequencies below 100 GHz [*Simmer*, 1994]. The microwave absorption for water vapor and oxygen is calculated according to *Rosenkranz* [1998], with adjustments in the water vapor continuum [*Turner et al.*, 2009] and for liquid water according to *Liebe et al.* [1991].

3.3. Derivation of Statistical Retrievals Using a Neural Network Approach

Statistical retrievals for LWP and mean layer r_{eff} are derived based on the data sets described in sections 3.1 and 3.2, which are divided into training and test parts. The training subset contains 70% of the original data set, and 15% are used for the testing and 15% for validation within the neural network retrieval development. In order to maintain the statistical properties, the original data set was divided randomly. This resulted in data sets with similar statistical properties. For example, the median LWP (r_{eff}) values for the training and testing data subsets are 28.52g/m^2 (6.0μm) and 29.79g/m^2 (5.9μm), respectively. Due to the limited sensitivity of the infrared methods, saturation occurs for LWP values larger than 40–60g/m^2. This nonlinear effect cannot be represented by a multivariate linear regression scheme. Therefore, a neural network (NNET) approach is chosen in this study. Since the infrared observations are saturated above 60g/m^2, they are only used in combination with the MWR. An overview of all retrievals that are derived and applied in this study is given in Table 3. In the following only the short names will be used.

Neural network retrievals have been widely used for cloud property retrievals [e.g., *Cadeddu et al.*, 2009; *Turner and Gero*, 2011]. The NNET architecture possesses the advantage of finding nonlinear statistical relationships between input parameters and target values [*Faure et al.*, 2001]. The network in this study consists of a two-layer feedforward network with sigmoid hidden neurons and linear output neurons. The input parameters p contain the linear and quadratic simulated brightness temperatures of the MWR (seven channels), the IRRs and the AERI radiances in the selected 13 microwindows. For the MWR 0.5 K was added to the brightness temperatures as random noise. The noise contributions for the simulated infrared radiances are 1 K (IRRs) and 0.2 mW (m^2 *sr* cm^{-1})$^{-1}$ (AERI). In the first layer (hidden layer), the input is weighted ($\mathbf{W_1}$) and a bias b_1 is added using the sigmoid function, giving an output a_1 in the range of 0 to 1:

$$a_1 = \text{logsig}(\mathbf{W}_1 p + b_1). \quad (5)$$

The weights and biases need to be adjusted in several iterations, in order to optimize the performance of the network in terms of the root-mean-square (RMS) error. In order to avoid overtraining, a validation set is used to decide when to stop the network training (according to *Hagan et al.* [2014]). The training set is used to compute the gradients and to determine the updated weight at each iteration. The error of the validation set is monitored during the training: if the error increases or remains the same for six iterations, the training is stopped. The testing data set is used as a further check that the network generalizes well. The number of weights and bias values can be adjusted to optimize the network performance. After testing several

Table 3. Neural Network Retrievals Developed in This Study

Instrument(s)	Variable	Short Name
MWR	LWP	MW_LWP
MWR + AERI	LWP	MW+AE_LWP
MWR + IRRs	LWP	MW+IR_LWP
MWR	r_{eff}	MW_reff
MWR + AERI	r_{eff}	MW+AE_reff
MWR + IRRs	r_{eff}	MW+IR_reff

configurations, the number was set to 20. In the second layer, the retrieval output a_2, which represents the LWP or r_{eff}, is computed with a linear transformation:

$$a_2 = \mathrm{lin}(\mathbf{W_2} a_1 + b_2). \quad (6)$$

The Levenberg-Marquardt algorithm was used for the back propagation in the MATLAB neural network toolbox, explained in detail in *Hagan et al.* [2014].

3.4. Setup of Shortwave Radiation Closure Study

While for the synthetic data study the retrieval performance can directly be evaluated, since the "truth" is known, it is more difficult to assess the retrieval performance using real measurements. To this end, a shortwave downwelling radiation closure study is performed (section 5). In this closure study, the measured shortwave radiation from the CMP 21 pyranometer at JOYCE is compared to the output of a broadband radiative transfer model using the retrieved LWP and r_{eff} as input. The deployed model is the broadband rapid radiative transfer model RRTMG, which has been developed by the Atmospheric and Environmental Research (AER) Incorporated [*Clough et al.*, 2005]. RRTMG provides accurate atmospheric fluxes and heating rates in the shortwave and longwave spectral regime and is widely used in numerical weather prediction and climate models. The accuracy has been extensively validated, in particular with comparisons between the RRTMG and the LBLRTM line-by-line calculations. The differences in shortwave fluxes in *Clough et al.* [2005] are found to be less than 1.5W/m^2 for the net flux in the troposphere. In the following, all crucial input variables used in this study are described in detail.

For the concentrations of ozone, methane, and oxygen, profiles of the midlatitude standard atmosphere are applied. Also, the thermodynamic profiles of temperature, pressure, and humidity from COSMO-DE are included. The effects of aerosols on the shortwave fluxes need to be accounted for. Therefore, vertical profiles of aerosol optical depth (AOD), single-scattering albedo, and asymmetry parameter are inserted in RRTMG. Values for the aerosol optical depths have been derived from AErosol RObotic NETwork (AERONET) [*Holben et al.*, 1998] measurements: The aerosol optical depths are calculated for all RRTMG midinterval wavelengths via the measured aerosol optical depths and Angstrom exponent at 870nm, which describes the spectral dependence of the aerosol optical depth. Here 870nm is taken as the reference wavelength, because of the high sensitivity to LWP in this spectral area. In this study a monthly mean AOD is assumed, which is vertically scaled using an exponential weighting function with a scaling height of about 1.3km. For the single-scattering albedo and the asymmetry parameter, values for urban aerosol are applied, which were computed from the Optical Properties of Aerosols and Clouds (OPAC) database [*Hess et al.*, 1998].

The direct-beam and diffuse shortwave surface albedo are included by using the Collection 5 products of the Terra and Aqua Moderate Resolution Imaging Spectroradiometer (MODIS) combined data set at 500 m resolution [*Schaaf et al.*, 2002].

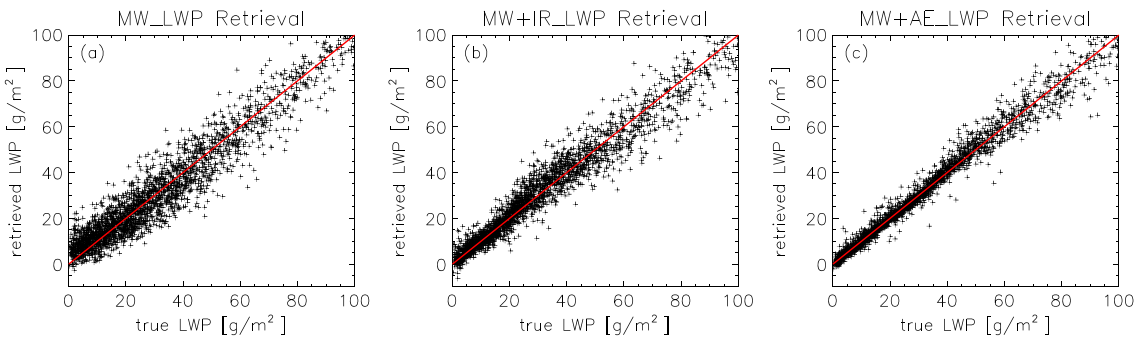

Figure 3. Scatterplots of the true (test data set) and retrieved LWP of the NNET-LWP retrievals (a) MW_LWP, (b) MW+IR_LWP, and (c) MW+AE_LWP. The legend describes the retrieval performance for low (LWP < 50 g/m^2) and high (LWP > 50 g/m^2) LWP situations to emphasize the different sensitivities of the infrared and microwave retrievals. The 1:1 line is given in red.

Table 4. Statistics (Correlation, Bias, and RMSE) for LWP and r_{eff} Retrievals of the Synthetic Study for LWP Values Below and Above 50g/m^2

	MW_LWP	MW+IR_LWP	MW+AE_LWP	MW_reff	MW+IR_reff	MW+AE_reff
LWP < 50 g/m^2						
Correlation	0.88	0.95	0.99	0.36	0.80	0.95
Bias	0.5g/m^2	1.0g/m^2	0.2g/m^2	0.04µm	−0.05µm	0.01µm
RMSE	6.5g/m^2	4.4g/m^2	2.4g/m^2	2.2µm	1.4µm	0.7µm
LWP > 50 g/m^2						
Correlation	0.996	0.996	0.997	0.35	0.55	0.62
Bias	−1.6g/m^2	−1.9g/m^2	−0.8g/m^2	−0.2µm	−0.1µm	0.02µm
RMSE	8.7g/m^2	9.1g/m^2	7.4g/m^2	1.8µm	1.6µm	1.5µm

4. Retrieval Test With Synthetic Data

In this section, the previously described retrievals for LWP and r_{eff} are tested with the simulated observations of MWR, AERI, and IRRs. Since the microwave and infrared spectral domains have distinct sensitivities for different LWP regimes, the performance of the single instrument and synergy retrievals is analyzed with respect to varying LWP values.

4.1. Retrieval Results for LWP

Comparing the MW_LWP retrieval to the synergy retrievals (MW+IR_LWP and MW+AE_LWP), the wide spread for low-LWP cases is noticeable in Figure 3a. If the IRR and AERI simulated radiances are combined with the MWR in the NNET approach, the benefit of the infrared domain is visible for low LWP values (Figures 3b and 3c). The absoulte root-mean-square error (RMSE) is reduced by 2.1g/m^2 for the MW+IR_LWP retrieval in the LWP range up to 50g/m^2 and by 4.1g/m^2 for the MW+AE_LWP retrieval (Table 4). In the range of higher LWP values, only the MWR and AERI synergy is able to improve the RMSE compared to the MWR-only retrieval (by 1.3g/m^2). Note that the axis range in Figure 3 was limited to 100g/m^2, but higher values do occur and the statistics in Table 4 encompass all values.

In order to get a better insight into the retrieval performance, the relative RMSE of the different retrievals is analyzed depending on the LWP for thin liquid water clouds up to 100g/m^2. Figure 4 shows a decrease in relative RMSE with increasing LWP for all retrievals. The expected high errors for the MW_LWP retrieval for low LWP values are also revealed, i.e., above 50%. At 100g/m^2 the relative error is decreased to around 8%. There is a distinct improvement for the combination of microwave and infrared simulated observations compared to the retrieval using only the MWR. Below 90g/m^2 the MW+AE_LWP retrieval shows a reduction in relative RMSE up to 37 percentage points (pp) compared to the MW_LWP retrieval results. For the entire LWP range of thin liquid water clouds, the MW+AE_LWP retrieval reveals the lowest relative RMSE of 7–17%, which translates into absolute errors of only 1.7–8.8g/m^2. Note that the relative error in the MW+AE_LWP retrieval, which uses a NNET retrieval approach, is almost identical to the relative error in the physical retrieval method of *Turner* [2007].

It has been demonstrated that the combination of the MWR and the highly spectrally resolved infrared measurements of the AERI are very beneficial in retrieving LWP. The question is if also the simulated broadband

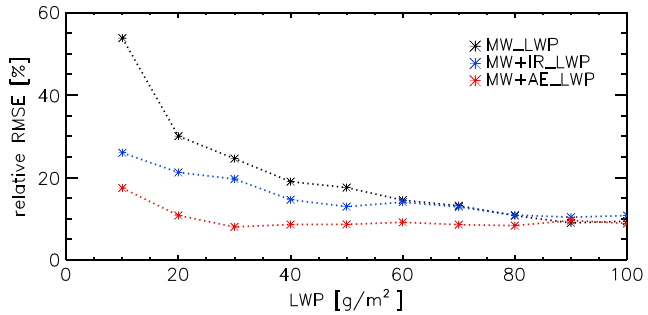

Figure 4. Relative root-mean-square error as a function of LWP for the different NNET-LWP retrievals.

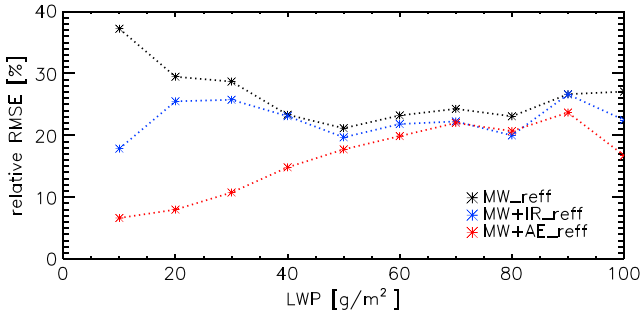

Figure 5. Relative root-mean-square error as a function of LWP for the different NNET r_{eff} retrievals.

infrared observations of the IRRs improve the MWR-derived LWP. In general, the relative RMSE increases if IRR instead of AERI observations are used (Figure 4). Replacing the AERI with the IRR simulated observations in a retrieval synergy leads to a reduced accuracy up to 9 pp in the retrieved LWP, with the larger impact at smaller LWP values. For the low LWP values the IRR and MWR retrieval combination still performs better than the MWR alone (up to 28 pp lower relative RMSE).

4.2. Retrieval Results for r_{eff}

In the following, the r_{eff} retrievals are discussed. In contrast to the NNET-LWP retrieval results in Figure 4, the RMSEs of the r_{eff} retrievals only show a strong dependence on the LWP for the MW+AE_reff retrieval (Figure 5). The RMSE increases from 0.7 below 50g/m^2 to 1.5 above 50g/m^2 (Figure 6c). As expected, the MWR observations reveal no sensitivity to r_{eff} (Figure 6a), which results in higher absolute errors of 1.3–2.4μm. However, the brightness temperatures are additionally used in combination with infrared measurements to retrieve r_{eff}, in order to examine if the MWR indirectly improves the r_{eff} estimation through constraining the LWP information.

For the MW+AE_reff retrievals a relative RMSE below 15% (absolute error = 0.4–0.8μm) can be seen up to 40g/m^2 in Figure 5, which is similar to the error only using the AERI (not shown). For higher LWP values, the combined retrieval MW+AE_reff shows an improvement of about 0.2μm. The average relative error of the MW+IR_reff retrieval is around 22.5% in the LWP range up to 100g/m^2. In terms of absolute errors the combination of IRR and MWR is on average 0.2μm lower than for the IRR alone. This implies that the brightness temperatures of the MWR provide some additional information to improve the r_{eff} retrieval accuracy via constraining the LWP. Using the spectrally highly resolved AERI observations instead of the broadband IRR ones, a significant improvement in the retrieval performance can be observed below 50g/m^2 (lower absolute error by 1.5μm).

5. Application to Real Measurements

With respect to synthetic data, the statistical NNET retrievals using the synergy of MWR and AERI show potential for retrieving LWP and r_{eff} for thin liquid water clouds. For this study it can be stated that the spectrally highly resolved AERI observations are favorable over the broadband IRR observations in a retrieval

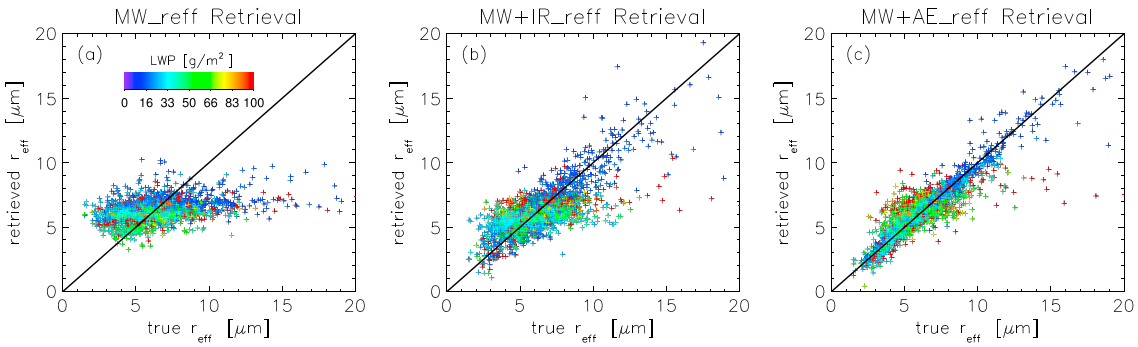

Figure 6. Same as Figure 3 for the NNET r_{eff} retrievals (a) MW_reff, (b) MW+IR_reff, and (c) MW+AE_reff. The data points are colored with the corresponding LWP from the test data set. The 1:1 line is given in black.

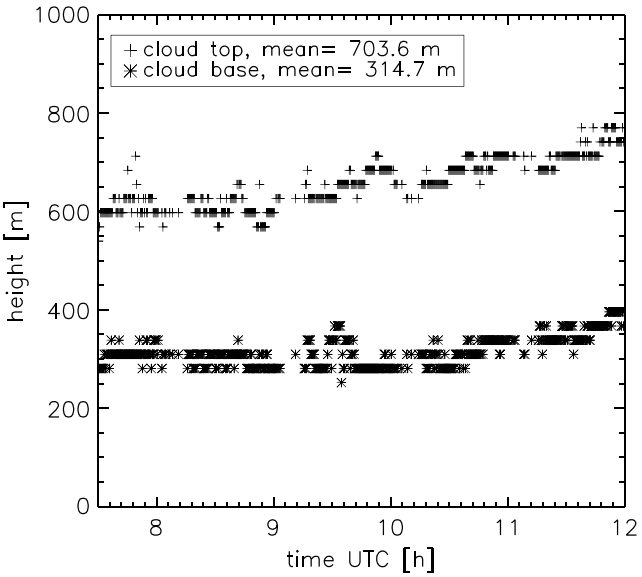

Figure 7. Cloudnet-derived cloud base and cloud top height. Results shown for 8 April 2015 (7.5–12 UTC).

combination with the MWR, especially for deriving the effective radius, although the combination of MWR and IRRs exhibits only a minor difference in retrieving the LWP compared to the MW+AE_LWP retrieval and displayed an improvement to the single instrument MWR retrieval. Thus, the LWP and r_{eff} retrievals of MWR, MWR+IR, and MWR+AERI have been chosen to be applied to real measurements at JOYCE. Since there is no truth for the cloud properties at JOYCE, the retrieval performance is evaluated in terms of a radiative closure study in this section. The focus is to show the potential of using both the LWP and r_{eff} retrievals for the closure.

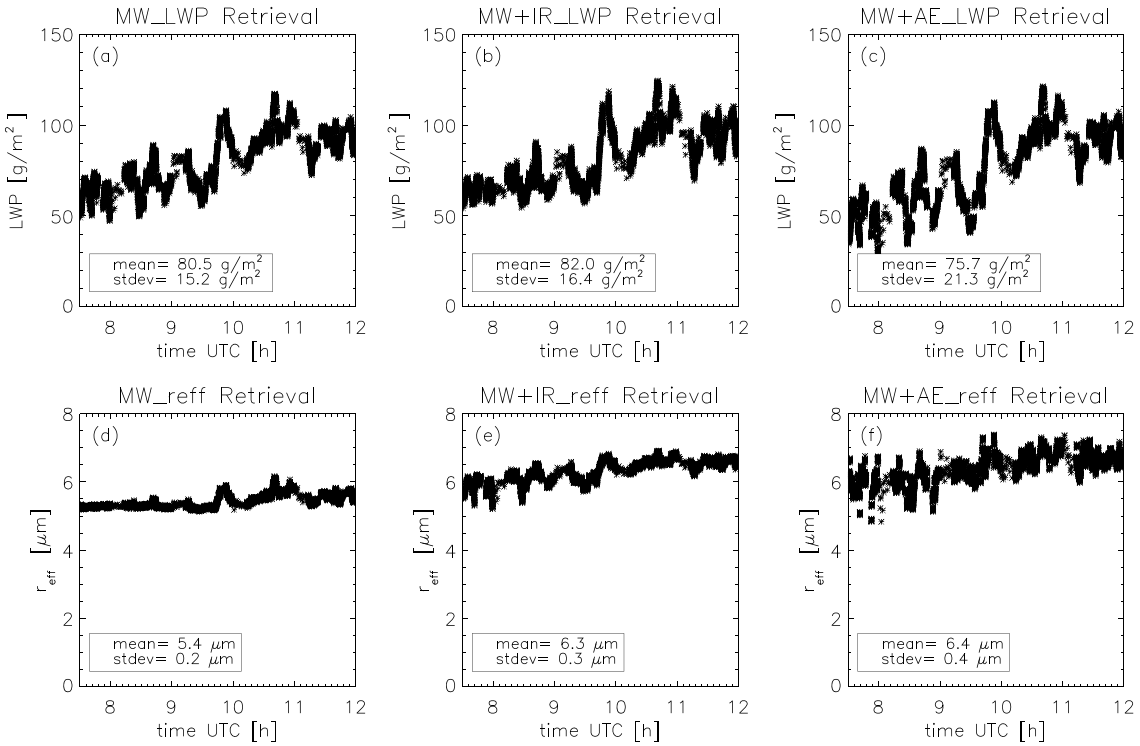

Figure 8. (a–c) LWP and (d–f) r_{eff} time series derived with the MWR (Figures 8a and 8d), MWR+IRR (Figures 8b and 8e), and MWR+AERI (Figures 8c and 8f) retrievals. Gaps in the measurements are due to MWR scans. Results shown for 8 April 2015 (7.5–12 UTC).

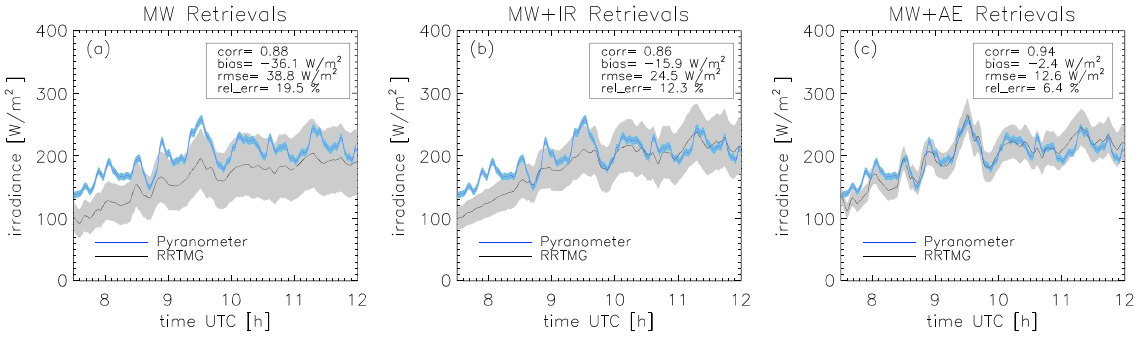

Figure 9. Time series for the RRTMG-derived shortwave downward flux (black line) averaged over 5 min and the measured shortwave downward flux for the CMP 21 pyranometer (blue line). (a) RRTMG calculation using the derived MW_LWP and MW_reff retrievals, (b) MW+IR_LWP and MW+IR_reff retrievals, and (c) MW+AE_LWP and MW+AE_reff retrievals. Shaded areas are due to measurement errors of the pyranometer and a LWP error of ±18% for the MW_LWP retrieval (MW+IR_LWP: ±14%, MW+AE_LWP: ± 9%). Results shown for 8 April 2015 (7.5–12 UTC).

5.1. Ideal Case Study Description

For the application of the retrievals to real measurements at JOYCE we will focus on a case on 8 April 2012 with a persistent single-layer liquid water cloud between 7.5 and 12 UTC (Figure 7). This time period of rather homogeneous cloud overcast condition has been chosen to minimize uncertainties in the radiative closure study due to three-dimensional radiation effects, which can introduce large errors in the shortwave radiation estimates based on 1-D radiative transfer calculations. Although the retrievals can be applied to broken cloud scenes, which are common for low-LWP scenes, they cannot be evaluated in this way. The derived LWP and r_{eff} from the NNET retrievals are used to calculate the shortwave flux in the radiative transfer model RRTMG.

The retrieved LWP values show an increase with time (Figures 8a–8c) corresponding to a higher cloud thickness. The lowest LWP mean value of 75.7g/m^2 and highest standard deviation (by about 6g/m^2) is retrieved by the MW+AE_LWP retrieval. The r_{eff} retrieval results are typically between 5 and 7μm and show a low variability. The combination of MWR and AERI (MW+AE_reff) shows the highest variations in r_{eff}, especially in the beginning of the time series where the LWP is still low. As expected, the MW_reff-derived r_{eff} is almost constant around 5.3μm, which is caused by the low sensitivity of the MWR to the r_{eff} (Figures 8d–8f).

5.2. Shortwave Radiative Closure Study

Since the shortwave fluxes of the CMP 21 pyranometer represent instantaneous hemispheric measurements, the calculated shortwave fluxes based on the cloud properties from the narrow field of view of AERI, IRR, and MWR are averaged over 5 min in order to improve the comparability. Using the derived LWP uncertainty from the synthetic data study, i.e., 18% for MW_LWP, 14% for MW+IR_LWP, and 9% for the MW+AE_LWP retrieval, the related bias error in the shortwave downwelling fluxes is assessed as an estimate for the uncertainty in the shortwave downwelling flux.

Using the MWR retrievals, a clear underestimation of the measured shortwave flux is visible (Figure 9a), resulting in a bias value of −36.1W/m^2. Adding broadband infrared observations in the LWP and r_{eff} retrievals (MWR+IRR approach), the calculated flux values are also lower than measured by the pyranometer, especially between 7.5 and 8.5 UTC. During this time, Figures 8b and 8e show higher LWP values combined with a lower variability in r_{eff} than in the MWR and MWR+AERI cases, causing the high negative bias. However, the MWR+IRR combination is still able to reduce the error in the shortwave flux to 12.3% compared to the RRTMG

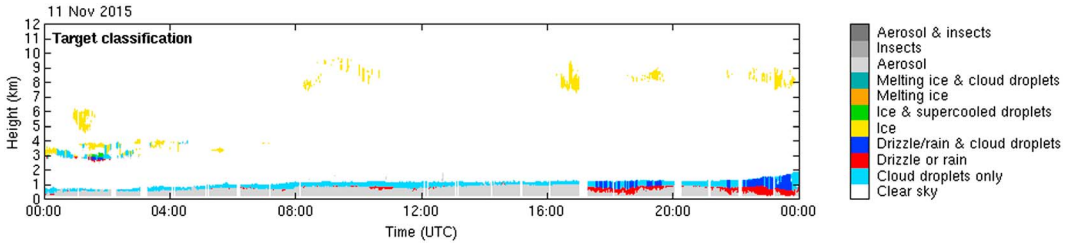

Figure 10. Cloudnet target classification for 11 November 2015. Gaps in the measurements are due to cloud radar scanning times.

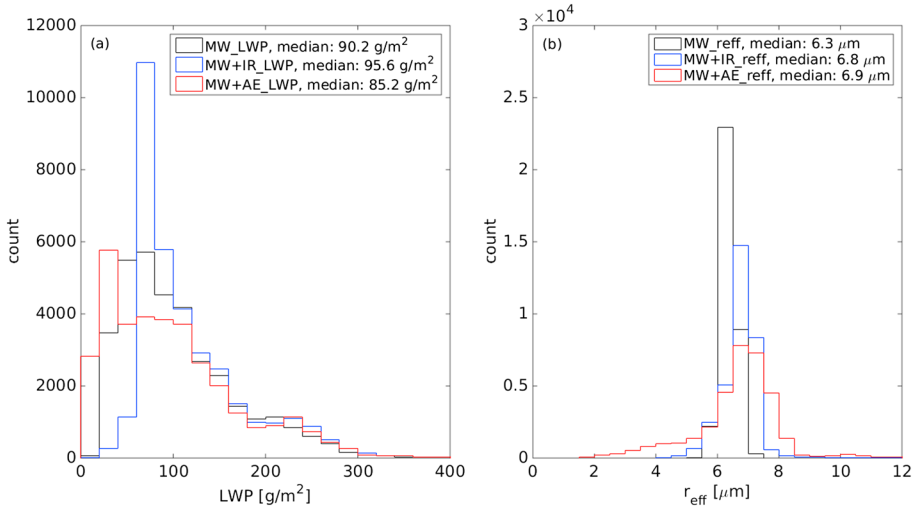

Figure 11. Histograms of (a) LWP and (b) r_{eff} derived with the MW (black), MW+IR (blue), and MW+AE (red) retrievals. Results shown for 11 November 2015 (0–24 UTC).

results using the MWR retrievals (relative RMSE of 19.5%). The derived shortwave downward flux using the MWR+AERI retrievals (Figure 9c) in the RRTMG calculations shows the best agreement within the retrieval uncertainties for the whole time period in comparison to the measured flux values (relative RMSE of 6.4%). The good shortwave closure for the MWR+AERI approach confirms the high accuracy for a combined retrieval using microwave and infrared observations for single-layer liquid water clouds with low LWP values.

5.3. Retrieval Robustness Analysis

In the previous section, an ideal case was selected to investigate the potential of the retrievals in a radiative closure study for a single-layer liquid water cloud. In order to demonstrate the robustness, the retrievals are applied to a full day of measurements including scenes which were not included in the retrieval training process (e.g., multilayer clouds, mixed-phase clouds, and drizzle; Figure 10). To increase the comparability, the MWR temporal resolution (1 s) was used for all LWP and r_{eff} retrievals for the whole day, resulting in 34,395 retrieved values.

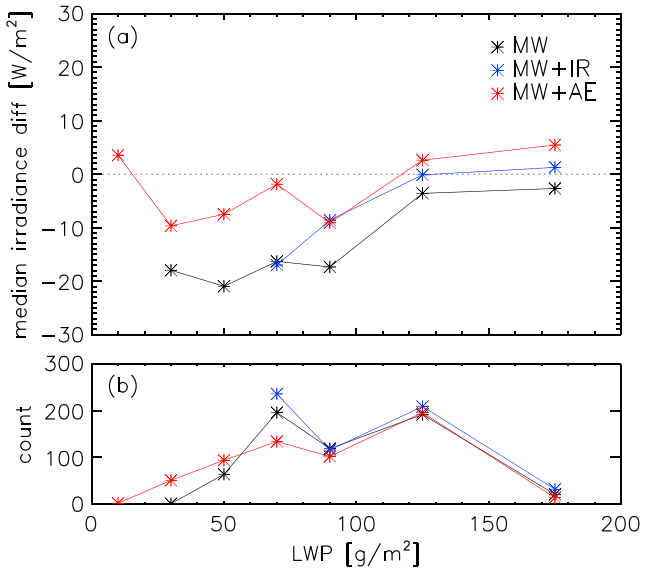

Figure 12. (a) Median calculated-observed shortwave irradiance difference (RRTMG − Pyranometer) and (b) number of occurrences as a function of LWP for the MW (black), MW+IR (blue), and MW+AE (red) retrievals. Results shown for 11 November 2015 (7–13 UTC).

The MW+AE_LWP retrieval provides the lowest values peaking at 10–20g/m^2, whereas the MW+IR_LWP and MW_LWP retrievals peak around 60–80g/m^2 and display a 5–10g/m^2 higher median (Figure 11a). For LWP values above 150g/m^2 all LWP distributions are in a similar range. The MWR+AERI combination also shows the broadest distribution for the retrieved r_{eff} values (Figure 11b). All median values are within 1μm, but the variability of the MW_reff and MW+IR_reff retrievals is much smaller, with no values below 4μm.

For the shortwave radiative closure study the time period from 7 UTC to 13 UTC was chosen due to sufficient sunlight and a measurement gap between 13 to 14 UTC. In this time period light drizzle and ice clouds were apparent. The differences of the computed and measured fluxes are analyzed in dependence of the retrieved LWP. For LWP below 80g/m^2 the MWR+AERI retrieval approach shows a clear improvement, first of all due to lower retrieved LWP values (Figure 12b) and with only a median difference around ±10W/m^2. In the range of higher LWP values, all retrieval approaches show a good closure. Above 100g/m^2, where the infrared methods are not improving the retrieval performance and the MWR information dominates, the retrieved LWP values of all retrievals fall within a 5% mean difference. The deviations between measured and calculated fluxes are thus caused by the higher uncertainty in the r_{eff}, with a 12% mean difference among the r_{eff} retrievals in this range.

6. Summary and Conclusions

Regarding the large impact of thin liquid water clouds on the interaction with radiation, there is a great demand for accurate retrieval representation of cloud microphysical properties. In this context, widely used microwave radiometer retrieval showed large uncertainties for low amounts of cloud liquid water. Therefore, the high sensitivity of the infrared spectral domain can be used to improve the retrieval performance in low-LWP situations.

In this study, we focused on statistical retrievals based on a neural network approach in order to retrieve microphysical properties of liquid water clouds using infrared and microwave observations. The derivation of robust and fast applicable LWP and r_{eff} retrievals for single-layer thin liquid water clouds (LWP < 100 g/m^2) was achieved using a synthetic data set of microwave observations and additional spectrally highly resolved and broadband infrared observations.

For the synthetic study, the retrievals based on the microwave and infrared synergy showed a high sensitivity and good performance for cases with low amounts of liquid water (relative error of 9–17%). In contrast, the MWR retrieval provides reasonable low errors beyond the point of saturation for the infrared retrievals (40–60g/m^2). For the combined microwave and infrared LWP retrievals, the application of simulated broadband IRR observations showed on average a 5 pp higher relative error compared to the spectral highly resolved ones from AERI but is still performing better than the MWR alone.

Considering the r_{eff} retrieval performance, the higher spectral resolution of the AERI infrared observations showed a clear improvement to the broadband IRR ones with a relative error below 20% (LWP < 60 g/m^2). As expected, there was no dependence on the r_{eff} for the microwave retrieval results, but the MWR brightness temperatures can still be used in combination with the infrared observations to improve the retrieval errors.

After applying the retrievals to real measurements at the Jülich Observatory for Cloud Evolution (JOYCE), the retrieval results need to be evaluated. In order to test the consistency of the retrieval results, a radiative closure study for the shortwave downwelling flux using a radiative transfer model (RRTMG) was performed. The best closure, compared to pyranometer measurements, is achieved for the MWR+AERI retrievals with only a 6.4% relative error in an ideal case. This retrieval also showed robust results for marginally invalid scenes, which encourages to include scenes which are currently not supported by the retrieval approach (e.g. clouds that partially fill the field of view of the instrument, mixed-phase clouds and drizzling clouds) in future studies. However, estimates of LWP are more uncertain and thus hard to interpret in complicated scenes. More detailed instrument system simulation experiments need to be conducted to fully understand the impacts of different "nonideal" physical conditions on the retrieval. For future field campaign deployments, independent observations of LWP and especially r_{eff} gathered from in situ or Sun photometer [*Chiu et al.*, 2012] measurements could help to further evaluate the retrievals and derive a more site-specific training data set of r_{eff}.

For the frequently occurring thin liquid water clouds, the neural network approach combining microwave and infrared observations can provide good estimates of the LWP and r_{eff} with orders of magnitude less computational demand compared to physical retrievals [*Turner*, 2007]. In order to apply the retrievals, only information

on the cloud phase must be available and nondrizzling water cloud cases need to be identified, since the training data set could only be derived for these conditions. Cloud phase determination can be obtained directly from the AERI [*Turner et al.*, 2003] or an additional data product like the Cloudnet algorithm, which is already available at many atmospheric supersites like JOYCE.

Acknowledgments

The authors would like to thank the Transregional Collaborative Research Center (TR32) "Patterns in Soil-Vegetation-Atmosphere Systems," which is funded by the German Science Foundation (DFG) and has continuously contributed to the instrumentation of JOYCE and its maintenance. Further, the Humidity And Temperature PROfiler (HATPRO) and the Atmospheric Emitted Radiances Interferometer (AERI) used in this study have been funded by DFG infrastructural programs under grants INST 216/681-1 and INST 216/519-1. Data management as well as the closure study were incorporated by the research initiative "High Definition Clouds and Precipitation for advancing Climate Prediction HD(CP)2 - Supersites" (first phase 2012–2016) funded by the German Ministry for Education and Research (BMBF). The work by Tobias Marke was funded by the TR32 project "Experimental study of spatiotemporal structures in atmosphere-land surface energy, water and CO_2 exchange (2014–2018)." The MODIS albedo MCD43A1.005 data product was retrieved from the online Data Pool, courtesy of the NASA Land Processes Distributed Active Archive Center (LP DAAC), USGS/ Earth Resources Observation and Science (EROS) Center, Sioux Falls, South Dakota. Access to the aerosol optical depths was made possible through AERONET and Birger Bohn from the Research Centre Jülich (b.bohn@fz-juelich.de).

References

Baldauf, M., and other (2011), *Kurze Beschreibung des Lokal-Modells Kürzestfrist LMK und seiner Datenbanken auf dem Datenserver des DWD*, German Weather Service (DWD) Geschäftsbereich Forschung und Entwicklung, 63004 Offenbach, Germany.

Boers, R., J. R. Acarreta, and J. L. Gras (2006), Satellite monitoring of the first indirect aerosol effect: Retrieval of the droplet concentration of water clouds, *J. Geophys. Res.*, *111*, D22208, doi:10.1029/2005JD006838.

Cadeddu, M. P., D. D. Turner, and J. C. Liljegren (2009), A neural network for real- retrievals of PWV and LWP from Arctic millimeter-wave ground-based observations, *IEEE Trans. Geosci. Remote Sens.*, *47*(7), 1887–1900, doi:10.1109/TGRS.2009.2013205.

Chiu, J. C., et al. (2012), Cloud droplet size and liquid water path retrievals from zenith radiance measurements: Examples from the atmospheric radiation measurement program and the aerosol robotic network, *Atmos. Chem. Phys.*, *12*, 10313–10329, doi:10.5194/acp-12-10313-2012.

Clough, S. A., M. J. Iacono, and J. L. Moncet (1992), Line-by-line calculations of atmospheric fluxes and cooling rates: Application to water vapor, *J. Geophys. Res.*, *97*(D14), 761–785, doi:10.1029/92JD01419.

Clough, S. A., M. W. Shepard, E. J. Mlawer, J. S. Delamere, M. J. Iacono, K. Cady-Pereira, S. Boukabara, and P. D. Brown (2005), Atmospheric radiative transfer modeling: A summary of the AER codes, *J. Quant. Spectrosc. Radiat. Transfer*, *91*, 233–244, doi:10.1016/j.jqsrt.2004.05.058.

Crewell, S., K. Ebell, U. Löhnert, and D. D. Turner (2009), Can liquid water profiles be retrieved from passive microwave zenith observations?, *Geophys. Res. Lett.*, *36*, L06803, doi:10.1029/2008GL036934.

Faure, T., H. Isaka, and B. Guillemet (2001), Neural network retrieval of cloud parameters of inhomogeneous and fractional clouds: Feasibility study, *Remote Sens. Environ.*, *77*, 123–138, doi:10.1016/S0034-4257(01)00199-7.

Frisch, A. S., C. W. Fairall, and J. B. Snider (1995), Measurement of stratus cloud and drizzle parameters in ASTEX with a K-band Doppler radar and microwave radiometer, *J. Atmos. Sci.*, *52*, 2788–2799.

Hagan, M. T., H. B. Demuth, M. H. Beale, and O. De Jesús (2014), *Neural Network Design*, 2nd edn., Oklahoma State Univ., Stillwater, Okla.

Hess, M., P. Koepke, and I. Schult (1998), Optical properties of aerosols and clouds: The software package OPAC, *Bull. Am. Meteorol. Soc.*, *79*, 831–844, doi:10.1175/1520-0477(1998)079<0831:OPOAAC>2.0.CO;2.

Holben, B. N., et al. (1998), AERONET—A federated instrument network and data archive for aerosol characterization, *Remote Sens. Environ.*, *66*, 1–16, doi:10.1016/S0034-4257(98)00031-5.

Hu, Y. X., and K. Stamnes (1993), An accurate parameterization of the radiative properties of water clouds suitable for use in climate models, *J. Clim.*, *6*, 728–742, doi:10.1175/1520-0442(1993)006<0728:AAPOTR>2.0.CO;2.

Illingworth, A. J., et al. (2007), Cloudnet continuous evaluation of cloud profiles in seven operational models using ground-based observations, *Bull. Am. Meteorol. Soc.*, *88*, 883–898, doi:10.1175/BAMS-88-6-883.

Intergovernmental Panel on Climate Change (2013), *Climate Change 2013: The Physical Science Basis. Contribution of Working Group 1 to the Fifth Assessment Report of the Intergovernmental Panel on Climate Change*, Cambridge Univ. Press, Cambridge, U. K.

Knist, C. L. (2014), *Retrieval of liquid water cloud properties from ground-based remote sensing observations*, dissertation at Delft Univ. of Technology, Delft, Netherlands.

Knuteson, R. O., et al. (2004a), Atmospheric emitted radiance interferometer. Part I: Instrument design, *J. Atmos. Oceanic Technol.*, *21*, 1763–1776, doi:10.1175/JTECH-1662.1.

Knuteson, R. O., et al. (2004b), Atmospheric emitted radiance interferometer. Part II: Instrument performance, *J. Atmos. Oceanic Technol.*, *21*, 1777–1789, doi:10.1175/JTECH-1663.1.

Krasnov, O. A., and H. W. J. Russchenberg (2002), An enhanced algorithm for the retrieval of liquid water cloud properties from simultaneous radar and lidar measurements, in *European Conference on Radar Meteorology (ERAD) 2002 Proceedings*, vol. 1, pp. 173–183, ERAD Publication Series, Delft, The Netherlands.

Kubar, T. L., D.-L. Hartmann, and R. Wood (2009), Understanding the importance of microphysics and macrophysics for warm rain in marine low clouds. Part I: Satellite observations, *J. Atmos. Sci.*, *66*, 2953–2972, doi:10.1175/2009JAS3071.1.

Liebe, H., G. Hufford, and T. Manabe (1991), A model for the complex permittivity of water at frequencies below 1 THz, *Int. J. Infrared Millimeter Waves*, *12*, 659–675, doi:10.1007/BF01008897.

Liljegren, J. C., E. E. Clothiaux, G. G. Mace, S. Kato, and X. Dong (2001), A new retrieval for cloud liquid water path using a ground-based microwave radiometer and measurements of cloud temperature, *J. Geophys. Res.*, *106*(D13), 485–500, doi:10.1029/2000JD900817.

Löhnert, U., and S. Crewell (2003), Accuracy of cloud liquid water path from ground-based microwave radiometry, 1. Dependency on cloud model statistics, *Radio Science*, *38*(3), 8041, doi:10.1029/2002RS002654.

Löhnert, U., S. Crewell, and C. Simmer (2004), An integrated approach toward retrieving physically consistent profiles of temperature, humidity, and cloud liquid water, *J. Appl. Meteorol.*, *43*, 1295–1307, doi:10.1175/1520-0450(2004)043<1295:AIATRP>2.0.CO;2.

Löhnert, U., et al. (2015), JOYCE: Jülich Observatory for Cloud Evolution, *Bull. Am. Meteorol. Soc.*, *96*, 1157–1174, doi:10.1175/BAMS-D-14-00105.1.

Marchand, R., T. Ackerman, E. D. Westwater, S. A. Clough, K. Cady-Pereira, and J. C. Liljegren (2003), An assessment of microwave absorption models and retrievals of cloud liquid water using clear-sky data, *J. Geophys. Res.*, *108*(D24), 4773, doi:10.1029/2003JD003843.

Miles, N. L., J. Verlinde, and E. E. Clothiaux (2000), Cloud droplet size distributions in low-level stratiform clouds, *J. Atmos. Sci.*, *57*, 295–311, doi:10.1175/1520-0469(2000)057<0295:CDSDIL>2.0.CO;2.

Rodgers, C. D. (2000), *Inverse Methods for Atmospheric Sounding: Theory and Practice*, 238 pp., World Scientific, Singapore.

Rose, T., S. Crewell, U. Löhnert, and C. Simmer (2005), A network suitable microwave radiometer for operational monitoring of the cloudy atmosphere, *Atmos. Res.*, *75*, 183–200, doi:10.1016/j.atmosres.2004.12.005.

Rosenkranz, P. W. (1998), Water vapor microwave continuum absorption: A comparison of measurements and models, *Radio Sci.*, *33*, 919–928, doi:10.1029/98RS01182.

Schaaf, C. B., et al. (2002), First operational BRDF, albedo nadir reflectance products from MODIS, *Remote Sens. Environ.*, *83*, 135–148, doi:10.1016/S0034-4257(02)00091-3.

Sengupta, M., E. E. Clothiaux, T. P. Ackerman, S. Kato, and Q. Min (2003), Importance of accurate liquid water path for estimation of solar radiation in warm boundary layer clouds: An observational study, *J. Clim.*, *16*, 2997–3009, doi:10.1175/1520-0442(2003)016<2997:IOALWP>2.0.CO;2.

Simmer, C. (1994), *Satellitenfernerkundung Hydrologischer Parameter der Atmosphäre mit Mikrowellen*, 13 pp., Verlag Dr. Kovac, Hamburg, Germany.

Stamnes, K., S.-C. Tsay, and K. Jayaweera (1988), Numerically stable algorithm for discrete-ordinate-method radiative transfer in multiple scattering and emitting layered media, *Appl. Opt.*, *27*, 2502–2509, doi:10.1364/AO.27.002502.

Stephens, G. L. (1978), Radiation profiles in extended water clouds. I: Theory, *J. Atmos. Sci.*, *35*, 2111–2122, doi:10.1175/1520-0469(1978)035<2111:RPIEWC>2.0.CO;2.

Stephens, G. L. (2005), Cloud feedbacks in the climate system: A critical review, *J. Clim.*, *18*, 237–273, doi:10.1175/JCLI-3243.1.

Turner, D. D. (2005), Arctic mixed-phase cloud properties from AERI lidar observations: Algorithm and results from SHEBA, *J. Appl. Meteorol.*, *44*, 427–444, doi:10.1175/JAM2208.1.

Turner, D. D. (2007), Improved ground-based liquid water path retrievals using a combined infrared and microwave approach, *J. Geophys. Rese.*, *112*, D15204, doi:10.1029/2007JD008530.

Turner, D. D., and P. J. Gero (2011), Downwelling 10 μm radiance temperature climatology for the Atmospheric Radiation Measurement Southern Great Plains site, *J. Geophys. Res.*, *116*, D08212, doi:10.1029/2010JD015135.

Turner, D. D., S. A. Ackerman, B. A. Baum, H. E. Revercomb, and P. Yang (2003), Cloud phase determination using ground-based AERI observations at SHEBA, *J. Appl. Meteorol.*, *42*, 701–715, doi:10.1175/1520-0450(2003)042<0701:CPDUGA>2.0.CO;2.

Turner, D. D., A. Shepard, J. C. Liljegren, E. E. Clothiaux, K. Cady-Pereira, and K. L. Gaustad (2007a), Retrieving liquid water path and precipitable water vapor from the Atmospheric Radiation Measurement (ARM) microwave radiometers, *IEEE Trans. Geosci. Remote Sens.*, *45*(11), 3680–3690, doi:10.1109/TGRS.2007.903703.

Turner, D. D., et al. (2007b), Thin liquid water clouds: Their importance and our challenge, *Bull. Am. Meteorol. Soc.*, *88*, 177–190, doi:10.1175/BAMS-88-2-177.

Turner, D. D., M. P. Cadeddu, U. Löhnert, S. Crewell, and A. M. Vogelmann (2009), Modifications to the water vapor continuum in the microwave suggested by ground-based 150-GHz observations, *IEEE Trans. Geosci. Remote Sens.*, *47*(10), 3326–3337, doi:10.1109/TGRS.2009.2022262.

Westwater, E. (1978), The accuracy of water vapor and cloud liquid determination by dual-frequency ground-based microwave radiometry, *Radio Sci.*, *13*, 667–685, doi:10.1029/RS013i004p00677.

Zhao, C., et al. (2012), Toward understanding of differences in current cloud retrievals of ARM ground-based measurements, *J. Geophys. Res.*, *117*, D10206, doi:10.1029/2011JD016792.